

Electron Correlations in Molecular Systems

Bogdan R. Bułka[†]

*Institute of Molecular Physics, Polish Academy of Sciences,
ul. Smoluchowskiego 17, 60-179 Poznań, Poland*

(January 16, 2018)

Abstract

A short review of correlated electrons in molecular systems has been performed. Main attention has been focussed on ET salts, which are the $d=2$ systems. They show the Mott transition in high temperatures and the transition from the antiferromagnetic to the superconducting phase in low temperatures, under a (chemical) pressure. Physical properties (the electrical resistivity, the specific heat, the magnetic susceptibility, the photoemission spectra, the optical conductivity) of ET salts have been compared with those ones in other strongly correlated systems. The optical conductivity is described in the framework of the Hubbard model, with a low frequency peak as an evidence for the Abrikosov-Suhl resonance.

I. INTRODUCTION

Recently we become more aware that interactions between electrons play an important role in many materials. Electron correlations in space and time, their fluctuations can be strong and therefore many physical properties are different than those for conventional metals described by a free electron picture. A list of materials with strongly correlated electrons, in which one can observe such differences, become longer and longer. Different types of materials are classified to the same class if kinetics of electrons is geometrically restricted to a d dimensional space. Despite their differences in a chemical composition, the materials of each class show similarities in many physical characteristics. Let us mention some of them.¹⁻³. Among $d=3$ correlated electron systems are: magnetic transition metals with 3d electrons, materials with the Mott type of the metal-insulator transition (e.g. V_2O_3), and heavy fermion systems (as UPt_3 , URu_2Si_2 , $CeAl_3$). If one extends the list to strongly correlated fermions, so liquid 3He should be placed there as well. With lowering dimensionality of the strongly correlated system their physical properties become more unusual, as those in high temperature superconductors with weakly coupled layer of conducting electrons. To the $d=2$ system one can classified also organic conductors and superconductors (e.g. ET salts, where $ET \equiv BEDT-TTF$ is bis(ethylenedithio)tetrathia-fulvalene), electronic systems showing a fractional quantum Hall effect and magnetic metallic multilayers. The so-called spin ladders are systems of localized spins and itinerant electrons, which dimensionality are closer to $d=1$ than $d=2$. Conducting polymers, organic conductors and organic superconductors are well known strongly correlated $d=1$ materials. There are also in this class inorganic

compounds with a charge density wave (CDW) and quantum wires as well edges of the $d=2$ systems in the quantum Hall effect. Due to developments in microtechnology we have also the $d=0$ systems as quantum dots and single electron transistors made of different materials.

Our knowledge on strongly correlated electrons increased significantly in recent 10 years. Enormous interest in high temperature superconductors gave also a new impact for studies of $d=2$ molecular systems. The aim of this paper is to review some of most interesting achievements in investigations of organic superconductors from the ET family.

The paper is organized in the following. We begin with a model description of some simple electron correlated systems. We show that the $d=2$ extended Hubbard model has the ground state with the antiferromagnetic phase (AF), the CDW or the superconducting phase of the s- and d- type pairing depending on interactions parameters. In high temperatures the system can be a metal or a Mott insulator. The physical quantities of the metallic phase can be derived within the Fermi liquid theory. The main part is an overview the properties of $(\text{ET})_2\text{X}$, where X= with X=Cu(NCS)₂, Cu[N(CN)₂]Br and Cu[N(CN)₂]Cl. The physical properties of the conducting $(\text{ET})_2\text{X}$ salts, as the electrical conductivity, the specific heat and the magnetic susceptibility, will be analyzed within the framework of the Fermi liquid theory. In this series of compounds the AF ordering and superconductivity of the d-type was found as well as the metal-insulator transition of the Mott type in high temperatures. We show photoemission studies of electronic structure and optical conductivity measurements, which indicate on strong correlations in these materials.

II. MODEL OF CORRELATED ELECTRONS AND ITS BASIC PROPERTIES

The hydrogen molecule H_2 is the simplest system with electron correlations. Let us remind that to describe a two electron state Slater postulated the wave function in the form⁴

$$\Psi_s(r_1, r_2) = \frac{1}{2}[\Phi_1(r_1)\Phi_1(r_2) + \Phi_1(r_1)\Phi_2(r_2) + \Phi_2(r_1)\Phi_1(r_2) + \Phi_2(r_1)\Phi_2(r_2)](\alpha_1\beta_2 - \alpha_2\beta_1) , \quad (1)$$

where $\Phi(r_m)$ is the single electron wave function for the m -th electron on the i -th atom and α_m, β_m are spinors describing spins up and down, respectively. The wave function el corresponds to free (uncorrelated) electrons. It is seen that in this basis the average for two electrons on a given hydrogen atom $\langle n_{1\uparrow}n_{1\downarrow} \rangle = \langle n_{1\uparrow} \rangle \langle n_{1\downarrow} \rangle = 1/4$. The Heitler-London wave function: function in the form⁴

$$\Psi_s(r_1, r_2) = \frac{1}{2}[\Phi_1(r_1)\Phi_2(r_2) + \Phi_2(r_1)\Phi_1(r_2)](\alpha_1\beta_2 - \alpha_2\beta_1) , \quad (2)$$

corresponds to the extreme strong correlations. In this case the average $\langle n_{1\uparrow}n_{1\downarrow} \rangle = 0$. It is well known⁴ that the exact solution for H_2 shows finite correlations with a wave function being the linear combination (1) and (2).

In the case of many electrons an exact solution is difficult to find. The simplest approximation used in such the case is the Hartree-Fock (HF) one

$$\langle a_{i\sigma}^\dagger a_{k\sigma'}^\dagger a_{l\sigma'} a_{j\sigma} \rangle \approx \begin{cases} \langle a_{i\sigma}^\dagger a_{j\sigma} \rangle \langle a_{k\sigma'}^\dagger a_{l\sigma'} \rangle & \text{for } \sigma = \sigma' , \\ \langle a_{i\sigma}^\dagger a_{j\sigma} \rangle \langle a_{k\sigma}^\dagger a_{l\sigma} \rangle - \langle a_{i\sigma}^\dagger a_{l\sigma} \rangle \langle a_{k\sigma}^\dagger a_{j\sigma} \rangle & \text{for } \sigma \neq \sigma' . \end{cases} \quad (3)$$

Here, $a_{i\sigma}$ denotes the annihilation operator of an electron with spin s at the i -th site of the lattice. This approximation for H_2 corresponds to the solution with the Slater wave function (1) and $\langle n_{1\uparrow} n_{1\downarrow} \rangle = \langle n_{1\uparrow} \rangle \langle n_{1\downarrow} \rangle = 1/4$. Electron correlations are neglected in the HF approximation. The exact results for the ground state energy can be significantly different from that one obtained within the HF approximation. For example, for a polyethylene chain the correlation energy, defined as $E_{corr} = E_{ground}^{exact} - E_{ground}^{HF}$, is -3.97 eV/monomer.². A simplest conducting polymer is polyacetylene $(CH)_x$. It is known that the Su-Schrieffer-Heeger model⁵ is not sufficient to describe quantitatively the physical properties of the $d=1$ chains of polyacetylene. It is needed to extend the model including local interactions of electrons. The Hamiltonian for $(CH)_x$ is given by

$$H = - \sum_{\langle i,j \rangle, \sigma} [t + (-1)^i 2\alpha\xi] c_{i\sigma}^\dagger c_{j\sigma} + U \sum_i n_{i\uparrow} n_{i\downarrow} + V \sum_{\langle i,j \rangle} n_i n_j + 2NK\xi^2 , \quad (4)$$

where the parameters determined in ab initio calculations are²: the hopping integral $t = 2.5$ eV, the electron-phonon coupling $\alpha = 40$ meV/pm, the elastic constant $K = 3.9$ meV/pm², the onsite Coulomb integral $U = 11.5$ eV, the intersite Coulomb integral $V = 2.4$ eV. The first term describes the kinetics of electrons in presence of the Peierls distortion ξ of the lattice, the last term is the elastic energy of the distorted lattice, the second and the third term correspond to the onsite and the intersite interaction of electrons. The electron-electron interactions in polyacetylene are moderately strong $U \approx W$ ($W = 4t$ is the width of the electronic band).

The tight binding Hamiltonian for interacting electrons on the lattice was first formulated and considered by Hubbard.⁶ It includes the kinetic term and the onsite interactions. The model described by (4) is called the extended Hubbard model, as it has additional terms. The extended Hubbard model with different intersite interactions has been recently intensively analyzed in hope to find an appropriate description of high temperature superconductors. Many physical properties in these materials indicate on strong electron correlations. The phase diagram oxide cuprates shows the AF ordering as well as the superconducting phase.⁷. Their relative stability depends on electron doping. Our studies⁸ of the stability of the ground state for the half-filled band of the $d=2$ extended Hubbard model performed within the HF approximation showed the AF ordering, if the onsite repulsion term dominates ($U > |V|$) - see Fig.1. For lower values of U the ground state stable solution is with CDW or superconducting, depending on the sign of the intersite coupling V . The superconducting state is the d-type symmetry for small negative values of V and a mixed s- and d-type, for larger couplings $|V|$.

Studies in finite temperatures are extremely difficult because one has to take into account, apart from correlations, various types of fluctuations in space and time. To overcome the problem one can analyze either in the limiting cases, of weak $U \ll t$ and strong onsite repulsion $U \gg t$, by means of the perturbation approach or using slave bosons. We performed the slave boson studies⁹ of the stability of the ground state with respect to the normal phase, which can be either metallic one or a Mott insulator, depending on the value of U . The slave boson approach includes electron correlations and give reliable results in

all range of U . The condensation energy and the critical temperature T_c for the AF phase increases with U , in the weak coupling limit, has a wide maximum at $U \approx W$ and decreases for large U .

The Mott transition to an insulating phase occurs in high temperatures only for the half-filled band. In the other cases the high temperature phase of a strongly correlated electron system is metallic, but its properties are different than those in conventional metals. The $d=1$ system of correlated electrons is described by the *Luttinger liquid* and in higher dimension ($d \geq 2$) by the *Fermi liquid*.² The concept of the Fermi liquid relies on the notion of quasiparticles, which have an energy spectrum ϵ_k and an effective relaxation time t . The Green's function, describing dynamics of quasiparticles, is

$$G(k, \omega) = \frac{1}{\omega - \epsilon_k^0 + \Sigma(k, \omega)} = \frac{Z}{\omega - \epsilon_k + i\hbar\tau^{-1}(\omega)} + G_{incoh}(k, \omega), \quad (5)$$

where $\Sigma(k, \omega)$ is a self-energy, $Z^{-1} = 1 - \partial\Sigma(k, \omega)/\partial\omega|_{\omega=0} = m^*/m$ is a renormalization constant, G_{incoh} is an incoherent part of the Green's function.

The function (5) can be used in derivations of many physical quantities, as the specific heat, different susceptibilities, and transport properties.² They involve low-energy excitations of the Fermi liquid. The excited electrons are close to the Fermi energy ϵ_F and the effective relaxation time is

$$\tau^{-1} = a(\omega - \epsilon_F)^2 + bT^2. \quad (6)$$

The electron mean free path due to electron-electron interaction is then $l_{el-el} = v_F\tau$, where v_F is the velocity at the Fermi energy. In low temperatures the electrical resistivity is therefore

$$\rho = \rho_0 + AT^2, \quad (7)$$

where ρ_0 is the residual resistivity. The specific heat is, in low temperatures, given by

$$C = \gamma T + \delta T^3 \ln T, \quad (8)$$

where $\gamma = k_B^2 m^* k_F / 3$ and k_F is the Fermi wave vector. The Sommerfeld coefficient γ as well as the effective mass m^* are enhanced due to correlations. The magnetic susceptibility is expressed

$$\chi = \chi_0 \frac{m^*/m}{S}, \quad (9)$$

where χ_0 is the magnetic susceptibility of free electrons and S is the Stoner enhancement factor, which plays an important role in magnetic properties of transition metals.

III. ELECTRON CORRELATIONS IN ET FAMILY

Recently Kanoda studied¹⁰ series of $(ET)_2X$ salts with $X=Cu(NCS)_2$, $Cu[N(CN)_2]Br$ and $Cu[N(CN)_2]Cl$ as well as their deuterated forms. All these salts are isostructural; they

are in the κ structure. From the temperature dependences of electrical resistivity, magnetic susceptibility, NMR as well as specific heat measurements Kanoda proposed¹⁰ the schematic phase diagram presented in Fig.2. The specific heat data for $(\text{ET})_2\text{Cu}[\text{N}(\text{CN})_2]\text{Br}$ showed¹¹ that a low temperature phase ($T < 13\text{K}$) is superconducting. Moreover, the dependence of the Sommerfeld coefficient γ in magnetic field is $\gamma(H) = A(H + H^*)^1/2$, what indicates on the superconducting phase with line of nodes.¹² In very low temperatures ($T < 1\text{K}$) the specific heat¹¹ exhibits an activated character suggesting on the s-type pairing as well. It means that the superconducting phase is the mixed s+d-type, with the d-component as a dominant one. The magnetic susceptibility data for $(\text{ET})_2\text{Cu}[\text{N}(\text{CN})_2]\text{Cl}$ showed¹³ at $T < T_N = 26 \div 27\text{K}$ an anisotropy of the susceptibility for a field perpendicular and parallel to magnetization - typical for the AF ordering (a small canting was also found in a direction parallel to the conducting layers). In the phase diagram, shown in Fig.2, $(\text{ET})_2\text{Cu}(\text{NCS})_2$ and $(\text{ET})_2\text{Cu}[\text{N}(\text{CN})_2]\text{Br}$ are on the metallic side, $(\text{ET})_2\text{Cu}[\text{N}(\text{CN})_2]\text{Cl}$ on the insulating side, and deuterated $(\text{ET})_2\text{Cu}[\text{N}(\text{CN})_2]\text{Br}$ just on the borderline. An applied pressure decreases the critical temperature T_c .¹⁰ The electronic bandwidth W increases with pressure and the ratio U_{eff}/W decreases (as the effective intradimer Coulomb repulsion U_{eff} is less sensible).

The phase diagram for the ET family (Fig.2) has a similar shape as that one for cuprates⁷, which has also the AF ordering close to the superconducting phase. However, in the present case the critical temperature is plotted vs. the ratio U_{eff}/W , whereas in cuprates it is a function of the electron concentration n . The electron concentration in the ET salts is always $n = 1$ (per a dimer, which is considered as an effective lattice site). The ratio U_{eff}/W is estimated to be close to unity.¹⁰ The diagram in Fig.2 is in agreement with the diagram of the ground state for the extended Hubbard model presented in Fig.1. If the considered system has the AF ordering, then with increasing pressure the value U/t decreases, while V/t remains unchanged. Thus, for $V/t < 0$ the system undergoes from the AF to the superconducting phase, which can be the s+d-type if the coupling is strong enough.

Photoemission spectroscopy of electrons is a direct measurement of dynamics of electrons and the Green's function (5). In the experiment one measures a spectral function $A(k, \omega)$ (or $B(k, \omega)$) by a direct (or an inverse) photoemission effect, which are expressed by

$$\text{Im}G(k, \omega) = -\pi A(k, \omega)\Theta(\omega - \varepsilon_F) + \pi B(k, \omega)\Theta(\varepsilon_F - \omega). \quad (10)$$

High-resolution photoemission studies were performed on the κ - $(\text{ET})_2\text{X}$ salts by Sekiyama et al. [14]. The photoemission spectra showed the electronic structure with many HOMO bands. In order to analyze a HOMO band with a smallest binding energy they extracted other bands from the photoemission spectra. In all investigated ET salts, the intensity is suppressed near eF, similarly as it was observed in various oxides,¹⁵ indicating on strong correlations of electrons. The spectra deviate from the HF calculations of the electronic structure. To explain the suppression of the intensity near ε_F , it was needed to assume a moderate mass renormalization for $(\text{ET})_2\text{Cu}[\text{N}(\text{CN})_2]\text{Cl}$ and a stronger renormalization for $(\text{ET})_2\text{Cu}(\text{NCS})_2$ and $(\text{ET})_2\text{Cu}[\text{N}(\text{CN})_2]\text{Br}$. It is contrast with the diagram proposed by Kanoda¹⁰, in which correlations are strongest in $(\text{ET})_2\text{Cu}[\text{N}(\text{CN})_2]\text{Cl}$.

According the Fermi liquid approach a low temperature resistivity should exhibit T^2 dependence [Eq.(7)] and its coefficient A has to be coupled with the coefficient γ in the specific

heat. Fig.3 collects the data for heavy fermion compounds, A15 materials, transition metals, fullerenes and organic conductors.¹⁶⁻¹⁹ The ratio $A/\gamma^2 = 1 \times 10^{-11} [\Omega cm(molK/mJ)^2]$ is universal value for heavy fermion systems (solid line in Fig.3) and $A/\gamma^2 = 4 \times 10^{-13}$ for transition metals (dashed line). Such two values are determined by Miyake et al. [16] as limiting ones for the Fermi liquid. Their approach¹⁶ was based on a phenomenological analysis of a frequency dependence of the self-energy $\Sigma(k, \omega)$ of the Green's function and its influence on A and γ . The value $A/\gamma^2 = 1 \times 10^{-11}$ is obtained for moderate many-body correlations, i.e. when $|\partial \text{Re}\Sigma(\omega)/\partial \omega| > 1$. If a large effective mass m^* of electrons is due to the properties of a single-body-band and $|\partial \text{Re}\Sigma(\omega)/\partial \omega| < 1$, then the ratio A/γ^2 is smaller and close to 4×10^{-13} .

The data for the organic compounds (full dots) lie in Fig.3 much above the solid line, the ratio A/γ^2 is much higher than the upper limit 1×10^{-11} . There are some explanations of this fact. A mechanism for T^2 dependence of the resistivity may be phononic (or libronic). In the presence of disorder and strong electron-phonon coupling the temperature dependence of the resistivity can be (after Gurvitch²⁰) proportional to T^2 . Other possibility is an error in determination of the coefficient A . In Fig.3 the diamonds represent the data for Sr_2RuO_4 ,¹⁸ which is a $d=2$ system with highly conducting planes. Precise measurements of the resistivity performed parallel and perpendicular to the conducting plane gave¹⁸ two different values of A (the points are denoted as \parallel and \perp in Fig.3, respectively). One may suspect that the presented data for the organic conductors were performed not precisely along the conducting plane (or chain) and they contained a perpendicular component as well. Precise measurements of the resistivity would show an anisotropy of A and new points in the plot A vs. γ would be placed lower than the present ones.

In Fig.4 the dependence of the Pauli susceptibility vs. the coefficient γ is presented for heavy fermion compounds, to which the data for the organic conductors and the metal oxides have been added. The points are close to the solid line corresponding to the Wilson ratio $R = \frac{\chi/\chi_0}{\gamma/\gamma_0} = 2$. It means that the organic conductors differ from single-body-band systems with $R = 1$, and correlations play an important role.

An analysis of optical properties of correlated metals is a much difficult task. The optical conductivity is expressed in terms of a current-current correlator $\langle [j, j] \rangle$ as

$$\sigma(\omega) = -\frac{1}{\omega} \text{Im} \langle [j, j] \rangle . \quad (11)$$

The function $\langle [j, j] \rangle$ describes dynamics an electron and a hole, and therefore, it is called as a two-particle Green's function. It is more difficult to determine the two-particle Green's function than the one-particle Green's function (5).

The formula (11) can be rewritten in the form²¹

$$\sigma(\omega) = -\frac{\langle T_x \rangle}{i\omega} - \frac{1}{i\omega} \sum_{n>0} \frac{|\langle n | J_{px} | 0 \rangle|^2}{\omega - (E_n - E_0) + i\hbar\tau^{-1}} . \quad (12)$$

Here, T_x and J_{px} denote the kinetic energy operator and the paramagnetic current operator along the current direction x , respectively. The sum is over all excited states n of the system. For a system with a discrete translation invariance (e.g. such as the Hubbard model) and for the relaxation time τ independent on the energy, one gets

$$\sigma(\omega) = -\frac{e^2 D}{Vd} \frac{\tau}{\pi} \frac{1}{1 + \omega^2 \tau^2} + \sigma_{incoh}(\omega), \quad (13)$$

where σ_{incoh} is an incoherent part of the conductivity, $D = \omega_p^{*2}/4\pi$ is a Drude weight and ω_p^* is a renormalized plasma frequency. In the limit $\omega \rightarrow 0$ one obtains from (12)

$$\frac{\omega_p^{*2}}{8} = -\frac{\pi}{2} \langle T_x \rangle - \pi \sum_{n>0} \frac{|\langle n | J_{px} | 0 \rangle|^2}{(E_n - E_0)}. \quad (14)$$

The integral

$$\frac{\omega_p^2}{8} \equiv \int d\omega \sigma(\omega) = -\frac{\pi}{2} \langle T_x \rangle \quad (15)$$

is the total oscillator strength (or the spectral weight). For noninteracting electrons the second term in (14) vanishes in the thermodynamic limit and therefore, $\omega_p^{*2} = \omega_p^2$ (as it is in the Drude model). For the model of interacting electrons the sum in (14) becomes nonzero and thus²¹

$$\omega_p^{*2} \leq \omega_p^2. \quad (16)$$

For all organic conductors the total oscillator strength ω_p^2 , calculated by integration of optical spectra, is significantly smaller than ω_p^{*2} , determined from the band edge.^{17,22} For example, in $(\text{ET})_2\text{Cu}(\text{NCS})_2$: $\omega_p^{*2} = 7.6 \times 10^{-7} \text{ cm}^{-2}$ and $\omega_p^2 = 4.9 \times 10^{-7} \text{ cm}^{-2}$ (for polarization of light parallel to the b-axis).¹⁷ An explanation of the controversy lies in oversimplified interpretation of optical spectra. Jacobsen²² and others used a single band model to description of measured spectra. They fitted the spectrum near the band edge to the Drude model [Eq.(13)]. The optical conductivity $\sigma(\omega)$ of organic conductors has a charge transfer band located at $2000 \div 4000 \text{ cm}^{-1}$ and a peak at low frequencies. Such the shape show also the optical data for $(\text{ET})_2\text{X}$ salts (X=Cu(NCS)₂ [23], Cu[N(CN)₂]Br [24] and Cu[N(CN)₂]Cl [25]). It does not seem particularly worthwhile to determine the parameters of the Drude model in the case of significantly different shape of optical conductivity as in ET salts (see also [24,25]).

Eldridge et al. [24] proposed to describe $\sigma(\omega)$ for $(\text{ET})_2\text{Cu}[\text{N}(\text{CN})_2]\text{Br}$ in terms of intra and inter-band transitions. They used²⁴ theoretical calculations of the electronic structure, which had been performed at $T=0$ and not taken electronic correlations into account. They could not explain temperature evolution of spectra, which showed a decrease of the intensity in low frequency range and increase of the intensity in the charge transfer band. $(\text{ET})_2\text{Cu}[\text{N}(\text{CN})_2]\text{Br}$ lies in the Kanoda phase diagram (Fig.2) close to the Mott transition. It resembles the situation studied by Pruschke et al. [26] for the Hubbard model of the infinite dimension. The electronic structure shows two overlapping bands, if the system is very close to the Mott transition from the metallic side. They found²⁶, in contrast to the result obtained by Hubbard²⁷, an additional resonant band exactly in the middle (the *Abrikosov-Suhl resonance*). The amplitude of the resonant band is temperature dependent and increases with $T \rightarrow 0$. The optical conductivity shows in this case the Drude peak as well as the CT band, which temperature intensities are mutual dependent. Since deuterated $(\text{ET})_2\text{Cu}[\text{N}(\text{CN})_2]\text{Br}$ is exactly on the border between the metal and the Mott insulator,

one expects to see the resonant band more pronounced (to our knowledge the experiment has not been performed). The effective mass m^* and other Fermi liquid parameters should be extremely large in this case.

IV. CONCLUSIONS

We have presented here a short review of physical properties of molecular systems with correlated electrons. Main attention has been focussed on a series of κ -(ET)₂X (X = Cu(NCS)₂, Cu[N(CN)₂]Br and Cu[N(CN)₂]Cl). Their phase diagram is qualitatively similar to that one for high temperature superconductors. A comparison with the other systems of correlated electrons showed that the effective mass m^* in the ET salts is a moderate value as well as the Sommerfeld coefficient γ . There are no experimental data on an increase of m^* when the system approaches to the Mott transition from the metallic side (i.e. in the salts with Cu(NCS)₂, Cu[N(CN)₂]Br and its deuterated form). The Wilson ratio in these compounds is $R \approx 2$ as in heavy fermions (Fig.4). Precise measurements of resistivity and its anisotropy are needed to determine the coefficient A . It would clarify the origin of correlations; whether they are a coulombic or a phononic nature. The photoemission data indicate on strong correlations¹⁴, but there is still lack of evidence for the Mott transition. The optical conductivity measurements show^{23,24} a flow of the spectral weight from the Drude peak to the CT band with increasing a temperature. One can assign it to changes of the intensity of the Abrikosov-Suhl resonance for the system close to the Mott transition.²⁶ We expect that an optical conductivity experiment for deuterated (ET)₂Cu[N(CN)₂]Br should give more evidence for the Mott transition.

In this lecture we did not present properties of $d=1$ organic compounds as (TMTTF)₂Y and (TMTSF)₂Y (with Y= PF₆, Br, ClO₄), which have many interesting properties.²⁸ For example, the phase diagram²⁸ has also the AF and superconducting phases and is similar to that one in Fig.2. Correlated electrons in the $d=1$ systems are analyzed within the Luttinger liquid theory. Their properties are different than those for the Fermi liquid. The one-particle Green's function is given then by

$$G(x, t) \propto \exp(ik_F x) \prod_{\alpha=\rho, \sigma} \frac{1}{[x - u_\alpha t + i/\tau]^{1/2+\eta_\alpha/2} [x + u_\alpha t - i/\tau]^{\eta_\alpha/2}}. \quad (17)$$

There is a separation of charge ρ and spin σ , which can move with different velocities u_ρ and u_σ . The form (17) is different than the Green's function (5) for the Fermi liquid. The function (17) has no real poles, what means that the picture of quasiparticles does not work in this case. Many physical properties are therefore different.²⁸

ACKNOWLEDGMENTS

The Committee for Scientific Research (KBN) has supported the work within the project No. 7T08A 003 12.

REFERENCES

- [†] E-mail address: bulka@ifmpan.poznan.pl
- ¹ N.F. Mott, *Metal Insulator Transition*, Taylor and Francis, London 1990.
- ² P. Fulde, *Electron correlations in Molecules and Solids*, Springer-Verlag. 1991.
- ³ A. Georges, G. Kotliar, W. Krauth and M.J. Rozenberg, *Rev. Mod. Phys.* 68, 13 (1996).
- ⁴ J. Slater, *Quantum Theory of Molecules and Solids*, vol.1, McGraw-Hill Book Company, 1963.
- ⁵ W.P. Su, J.R. Schrieffer, A.J. Heeger, *Phys. Rev. Lett.* 42, 1698 (1979); *Phys. Rev.* B22, 2099 (1980).
- ⁶ J. Hubbard, *Proc. Roy. Soc. London* A276, 238 (1963).
- ⁷ E. Dagatto, *Rev. Mod. Phys.* 66, 763 (1994) and references therein.
- ⁸ B.R. Bulka, *Phys. Stat. Solidi* b163, 197 (1991); *Physica* B165-166, 1037 (1990).
- ⁹ B.R. Bulka and S. Robaszkiewicz, *Phys. Rev.* B54, 13138 (1996); B. R. Bulka, *Phys. Rev.* B57, 10303 (1998).
- ¹⁰ K. Kanoda, *Hyperfine Interact.* 104, 235 (1997); *Physica* C282-287, 299 (1997).
- ¹¹ Y. Nakazawa and K. Kanoda, *Phys. Rev.* B55, 8670 (1997).
- ¹² G.E. Volovik, *JETP Lett.* 58, 469 (1993).
- ¹³ K. Miyagawa, A. Kawamoto, Y. Nakazawa and K. Kanoda, *Phys. Rev. Lett.* 75, 1174 (1995).
- ¹⁴ A. Sekiyama, T. Susali, A. Fujimori, T. Dasaki, N. Toyota, T. Kondo, G. Saito, M. Tsunekawa, T. Iwasaki, T. Mura, T. Mutsushita, S. Suga, H. Ishii and T. Miyahara, *Phys. Rev.* B56, 9082 (1997).
- ¹⁵ A. Fujimori et al., *Phys. Rev. Lett.* 69, 1796 (1992).
- ¹⁶ K. Miyake, T. Matsuura and C. M. Varma, *Solid State Comm.* 71, 1149 (1989).
- ¹⁷ M. Dressel, G. Gruner, J. E. Eldridge and J.M. Williams, *Synth. Met.* 85, 1503 (1997).
- ¹⁸ Y. Maeno et al., *J. Phys. Soc. Jpn* 66, 1405 (1997).
- ¹⁹ Y. Tokura, Y. Taguchi, Y. Okada, Y. Fujishima, T. Arima, K. Kumagi and Y. Iye, *Phys. Rev. Lett.* 70, 2126 (1993).
- ²⁰ M. Gurvitch, *Physica* B135, 276 (1985).
- ²¹ W. Kohn, *Phys. Rev.* 133, A171 (1964); A.J. Millis and S.N. Coppersmith, *Phys. Rev.* B42, 10807 (1990).
- ²² C.S. Jacobsen, *J. Phys.* C19, 5643 (1986).
- ²³ K. Kornelsen, et al., *Solid State Comm.* 72, 475 (1989).
- ²⁴ J.E. Eldridge, et al., *Solid State Comm.* 79, 583 (1991).
- ²⁵ K. Kornelsen et al., *Solid State Comm.* 81, 343 (1992).
- ²⁶ Th. Pruschke, D.L. Cox and M. Jarrell, *Phys. Rev.* B47, 3553 (1993).
- ²⁷ J. Hubbard, *Proc. Roy. Soc. London* A281, 401 (1964).
- ²⁸ D. Jerome, in *Organic Conductors*, ed. J-P. Farges, Marcel Dekker, Inc. , New York 1994; J.Moser, M. Gabay, P. Auban-Senzier, D. Jerome, K. Bechgard and J.M. Fabre, *Eur. Phys. J.* B1, 39 (1998); C. Bourbonnais, *Synth. Met.* 84, 19 (1997); and references therein.

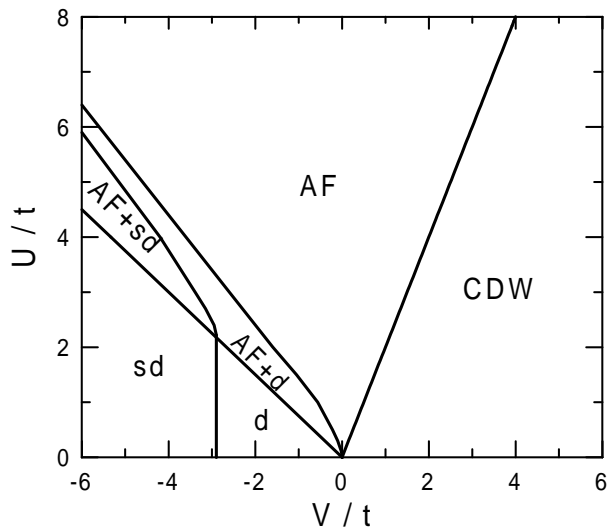


Fig.1

The phase diagram in the space of the parameters U (onsite interaction) and V (intersite density-density interaction) of the $d=2$ extended Hubbard model determined within the HF approximation for the half-filled band (the electron concentration $n=1$) at temperature $T = 0$. There are denoted the regions of the antiferromagnetic (AF), the charge density wave (CDW) and the superconducting state of the d-type (d) and the mixed s and d-type pairing (sd). Superconductivity and AF can coexist (in the region denoted AF+sd and AF+d) (after [8]).

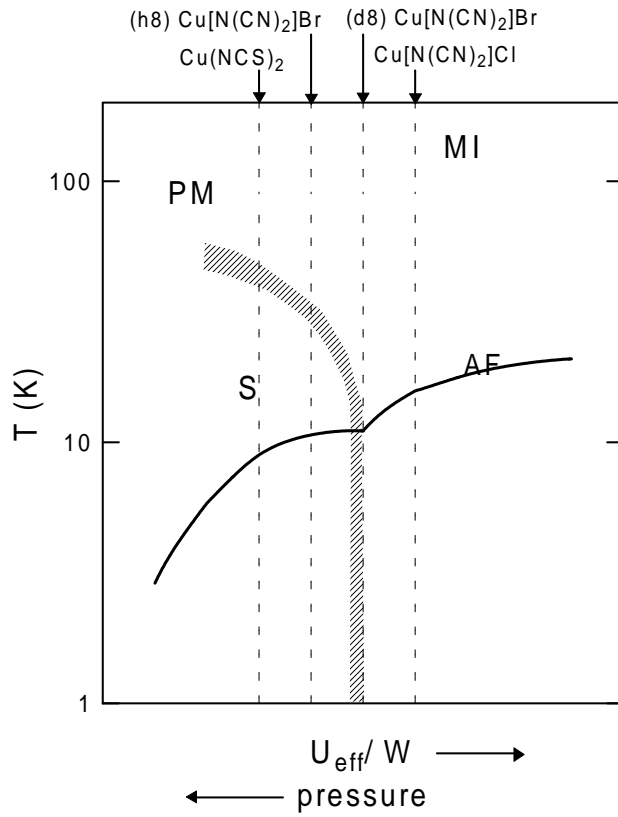


Fig.2

Schematic phase diagram for κ -(ET)₂X with X= $\text{Cu}(\text{NCS})_2$, $\text{Cu}[\text{N}(\text{CN})_2]\text{Br}$, $\text{Cu}[\text{N}(\text{CN})_2]\text{Cl}$ and deuterated $(\text{ET})_2\text{Cu}[\text{N}(\text{CN})_2]\text{Br}$ denoted as $(d8) \text{Cu}[\text{N}(\text{CN})_2]\text{Br}$. The regions for the superconducting, the antiferromagnetic, the paramagnetic metal as well as the Mott insulator phase are denoted as S, AF, PM and MI, respectively. (after [10]).

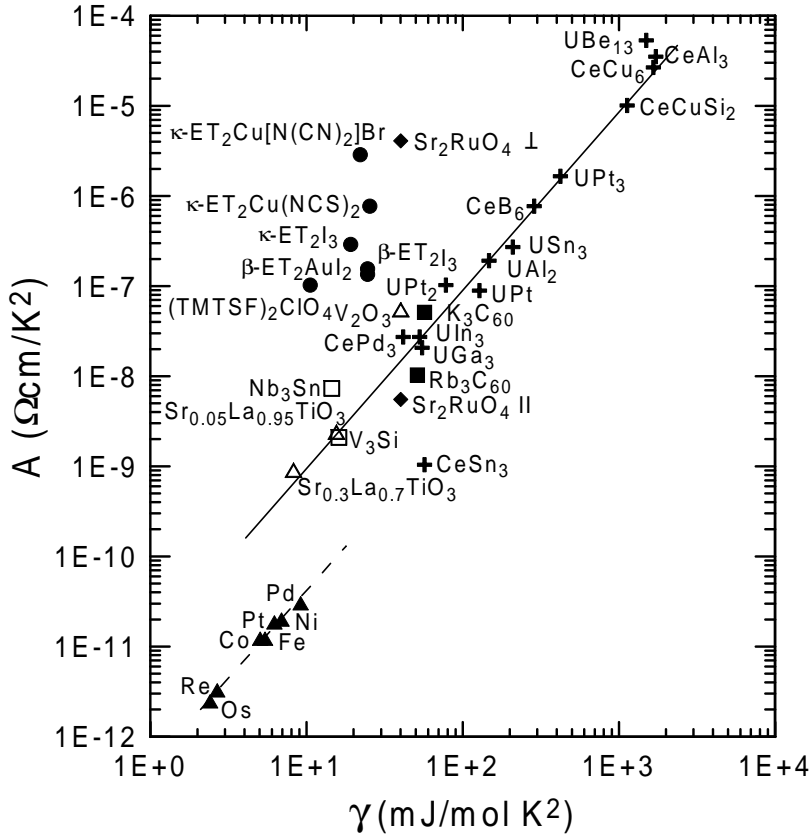


Fig.3

Resistivity coefficient A plotted vs. the Sommerfeld coefficient γ for heavy fermion systems (crosses), fullerenes (full boxes), A15 superconductors (open boxes), metal oxides (open triangles), organic conductors (dots) and transition metals (full triangles) (after [16,17,19]). Diamonds denote the data for Sr_2RuO_4 measured in a direction parallel (\parallel) and perpendicular (\perp) to the conducting plane (after [18]).

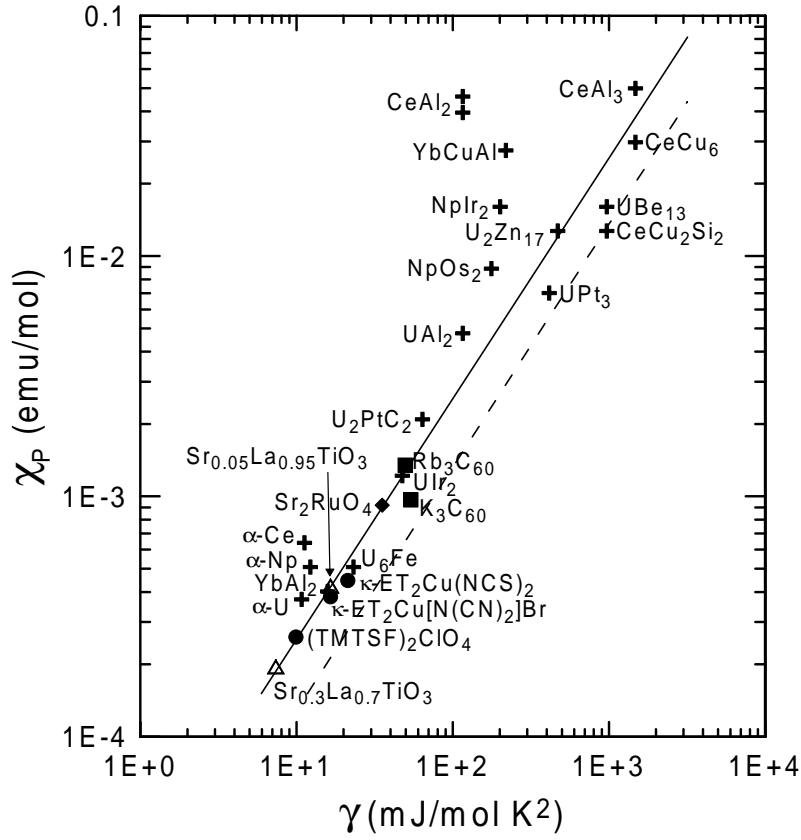


Fig.4

Pauli susceptibility plotted vs. the Sommerfeld coefficient γ for heavy fermion systems (crosses) [18], metal oxides (open triangles) [19] and organic conductors (dots). Diamond denotes the point for Sr_2RuO_4 (after [18]). The solid and dashed lines correspond to the Wilson ratio $R = 2$ and 1, respectively.